

Mesoscopic simulation of self-assembly of carbon nanotubes into a network of bundles

Alexey N. Volkov^{*}, Kiril R. Simiov[†], and Leonid V. Zhigilei[‡]

*Department of Materials Science and Engineering, University of Virginia
395 McCormic Rd., Charlottesville, VA, 22904-4745*

A computational approach for generation of network structures of interconnected carbon nanotube (CNT) bundles, commonly observed in CNT-based materials, is developed and tested. The approach is based on a mesoscopic computational model designed for simulation of large systems of interacting CNTs. The model adopts a coarse-grained representation of a CNT as a sequence of stretchable cylindrical segments defined by a chain of nodes. The dynamic behavior of CNTs is reproduced with the help of a mesoscopic force field, by solving the equations of motion for the nodes. The mesoscopic force field accounts for stretching and bending of individual CNTs, as well as for the van der Waals interactions among the nanotubes. Simulations, performed for systems containing thousands of CNTs and having dimensions on the order of a micrometer, predict spontaneous self-assembly of CNTs into a continuous network of bundles. The structures produced in the simulations are qualitatively similar to the structures of CNT films and mats observed in experiments.

Nomenclature

R_T	=	radius of carbon nanotubes
x, y	=	Cartesian coordinates in the film plane
z	=	Cartesian coordinate in the direction normal to the film plane
t	=	time
\mathbf{r}	=	position vector
E	=	kinetic energy
U	=	potential energy

I. Introduction

The severe operating conditions combined with stringent weight requirements define a challenging task of designing robust ablative shield materials capable, in addition to the thermal protection, of mitigating various hazardous effects characteristic of the space environment and serving as a structural component.¹ CNT-reinforced polymer matrix nanocomposites present an increasingly competitive alternative to conventional polymer composites^{2,3} and have a potential for meeting the challenge of multi-functionality. Heat shielding and structural functions of nanocomposite materials can be enabled by the ability of CNTs to form low weight high mechanical strength polymer matrix composites.^{4,5} A significant enhancement of the dynamic mechanical strength of CNT-phenolic nanocomposite with CNTs arranged in a continuous network has been recently demonstrated,⁶ suggesting a potential use of the nanocomposite for protection from hypervelocity impacts by meteoroids, space debris and energetic particles.^{7,8} Low atomic weight of the material components and the ability to fine-tune the density and composition by functionalizing or filling the nanotubes with various molecules^{9,10} make the nanocomposite material to be appropriate for radiation shielding.¹

^{*} Research Scientist, Member AIAA

[†] Graduate Student

[‡] Associate Professor

Computational investigation of CNT-based materials has a potential for playing an important role in designing nanocomposite materials with properties tailored for thermal protection systems in aerospace vehicles. A model capable of predicting the effective thermal and mechanical properties of a nanocomposite material should include a sufficiently large number of structural elements constituting the material. In CNT-based composites and “pure” (without matrix) CNTs materials, CNTs are typically arranged into bundles or ropes.^{11,12,13} The microscopic structure of these materials is, therefore, defined by the spatial arrangement of bundles rather than nanotubes themselves. The typical size of pores in a network of CNT bundles is on the order of hundreds of nanometers and the bundle length can be as large as hundreds of microns.^{11,14,15} Hence, in order to study the macroscopic properties of CNT-based materials, it is necessary to develop an approach capable of reproducing a realistic structure of CNT bundles at a length scale of micrometers.

The goal of this paper is to develop a computational approach for simulation of a random network of CNT bundles at a realistic length scale. The approach is based on a mesoscopic representation of individual CNTs, proposed in Ref. 16, and a novel computationally-efficient “tubular” potential for simulation of the van der Waals interaction among nanotubes, briefly discussed in Ref. 17. The results of the simulations performed in this work for pure CNT materials, such as nanotube mats (bucky paper)^{11,12,13} and films,^{18,19,20} demonstrate the ability of the model to describe the structural evolution in the material at the mesoscopic level and provide a solid foundation for future extension of the model to the investigation of the mechanical and thermal (including charring²¹) behavior of CNT-reinforced polymer matrix nanocomposites.

II. Discrete mesoscopic model for carbon nanotubes

The model used in this work is based on the mesoscopic approach proposed in Ref. 16. Every CNT is represented as a chain of cylindrical segments, with each segment described by coordinates of its ends (or nodes). The interactions among the segments are described by a mesoscopic force field. The force field used in this work includes a description of stretching and bending of individual CNTs, as well as non-bonding interactions among the CNTs. This simplified force field is sufficient for simulations of spontaneous self-assembly of CNTs, investigated in this work. Other aspects of the physical behavior of CNTs, such as buckling, fracture, dynamic variation of radii, and torsional dynamics can be activated in the mesoscopic model if needed for the description of processes involving large deformations or dynamic loading.

Below we provide a brief description of the general idea of the mesoscopic model, with full details and parameters given elsewhere.^{16,17,22} In a system of N CNTs, each nanotube i ($i = 1, \dots, N$) is represented by N_i nodes (including two end nodes). The state of the nanotube i can be characterized by a set of position vectors $\mathbf{r}_{i,j}$ of its nodes, $\mathbf{R}_i = (\mathbf{r}_{i,1}, \dots, \mathbf{r}_{i,N_i})$, so that the pair $(\mathbf{r}_{i,j}, \mathbf{r}_{i,j+1})$ defines the position and orientation of segment j of the nanotube i . The dynamics of the system can be described by the equations of motion of classical mechanics in the Lagrangian form

$$\frac{d}{dt} \frac{\partial L}{\partial \dot{\mathbf{R}}} - \frac{\partial L}{\partial \mathbf{R}} = 0, \quad (1)$$

where $\mathbf{R} = (\mathbf{R}_1, \dots, \mathbf{R}_i, \dots, \mathbf{R}_N)$, $\dot{\mathbf{R}} = d\mathbf{R}/dt$, $L = E(\dot{\mathbf{R}}) - U(\mathbf{R})$ is the Lagrangian of the system, E and U are the kinetic and potential energies of the system. In the model considered in this work, the only motion is the translational motion of nanotube nodes and, therefore, the kinetic energy of the system is equal to

$$E(\dot{\mathbf{R}}) = \sum_{i=1}^N \sum_{j=1}^{N_i} \frac{m_{i,j}}{2} (\dot{\mathbf{r}}_{i,j})^2, \quad (2)$$

where $m_{i,j}$ is the mass of a part of nanotube i represented by node j . The potential energy of the system, $U(\mathbf{R})$, is defined as

$$U(\mathbf{R}) = U_{\text{Str}}(\mathbf{R}) + U_{\text{Bnd}}(\mathbf{R}) + U_{\text{Int}}(\mathbf{R}), \quad (3)$$

where $U_{\text{Str}}(\mathbf{R})$, $U_{\text{Bnd}}(\mathbf{R})$, and $U_{\text{Int}}(\mathbf{R})$ are the potential energies of nanotube stretching, bending, and inter-tube interactions, respectively.

Terms $U_{\text{Str}}(\mathbf{R})$ and $U_{\text{Bnd}}(\mathbf{R})$ in Eq. (3) are defined by harmonic potentials parameterized in Ref. 16 based on the results of atomistic simulations performed with the Reactive Empirical Bond-Order potential (REBO).^{23,24} Inter-tube interaction energy, $U_{\text{Int}}(\mathbf{R})$ in Eq. (3), is calculated with the help of a tubular potential method proposed in Refs. 17 and 22 for simulation of the interaction between arbitrary mesoscopic tubular particles. This method consists of two

main parts. The first part is a new computationally-efficient “tubular potential” describing the interaction between a cylindrical segment and an infinitely-long or semi-infinite straight nanotube. In contrast to existing potentials of such kind,^{25,26} that can be applied to the description of parallel infinitely-long tubes only, the developed tubular potential is valid for an arbitrary relative orientation and position of a cylindrical segment with respect to a tube. The potential is parameterized based on an interatomic potential describing the van der Waals interaction between a pair of carbon atoms.²⁷ The second part of the model is a weighted approach allowing us to apply the tubular potential for calculation of interactions between tubes of arbitrary curvature.^{17,22}

III. Generation of a random network of CNT bundles in CNT-based materials

One of the challenges in modeling of CNT-based nanocomposite materials is the preparation of the initial system with a complex random structure of CNT bundles, similar to the ones observed in experiments.^{12-15,18,19} The direct generation of a continuous network of CNT bundles is a difficult task. Moreover, due to the irregular nature of the nanocomposite structure and limitations of the methods of material characterization, the methodology for quantitative description of these random structures is still at the stage of initial development.^{14,15,28}

In this paper, we propose an approach for generation of random CNT bundle structures that, at least partially, mimics the actual process of bundle formation in experiments. This approach consists of two stages.

At the first stage, we generate an initial sample consisting of individual nanotubes that are not arranged into bundles. The properties of the sample at this stage are characterized by statistical properties of individual tubes (distributions of their radii, lengths, and shapes) and parameters governing their distribution in the sample (density and homogeneity of the material, degree of anisotropy in CNT orientation, etc).

At the second stage, we allow the system of CNTs to evolve freely in the course of a dynamic simulation performed with mesoscopic model briefly discussed in the previous section. The simulation is performed at an elevated temperature and is continued until a network of CNT bundles with desired morphology is generated. Then this structure of bundles is quenched or kept quasi-static in thermostat at a sufficiently low (e.g. 300 K) temperature. The process of CNT self-organization into bundles can be steered by controlling pressure and kinetic energy in the system.

Within the framework of this approach, the final structure of the network of CNT bundles is defined by a set of parameters controlling the initial distribution of the individual nanotubes at the first stage of the sample preparation and the conditions of the dynamic simulation at the second stage.

IV. Generation of initial samples

The initial distribution of individual CNTs in the sample was constructed using two different algorithms or *Generators*.

In *Generator I*, the nanotubes are grown within the computational cell from randomly selected “seed segments” in a “segment-by-segment” manner. Positions and orientations of new segments, attached to ones already included into the sample, are chosen with the help of a random “trial-and-error” method designed to keep the total energy of the sample at a low level. This method produces a random three-dimensional structure of slightly curved nanotubes. The algorithm ensures, if necessary, spatial periodicity of the sample in any direction. *Generator I* was used in Ref. 17 to prepare the initial distributions of short (18 nm long) CNTs in relatively small (60 nm × 60 nm × 60 nm) samples with densities up to 0.15 g/cm³. It was found that this algorithm is highly inefficient for generation of large dense samples consisting of longer CNTs. Moreover, the desired density can be unachievable with this algorithm, as at some stage of the sample generation an addition of the next CNT can become impossible.

In order to overcome these difficulties, an alternative method (*Generator II*) is developed. It exploits the “deposition-like” approach, which mimics the process of deposition of CNTs on a substrate. Technically, there are several ways to implement this approach. In particular, the deposition of each nanotube can be followed by the energy minimization involving changes in shapes and positions of the deposited CNTs.

In this paper, the “deposition-like” technique is used in its simplest form, where all nanotubes are assumed to be straight and the initial sample consists of a stack of parallel “layers” of nanotubes. Within each layer, the axes of all CNTs belong to the plane of the layer. The layers are separated from each other by a distance of $2R_T + \delta_L$, where R_T is the radius of the CNTs, $\delta_L < r_c$, and r_c is the cutoff distance of the tubular potential. The restriction on the value of δ_L ensures some degree of interaction between tubes that belong to different layers.

The distributions of nanotubes in different layers are generated independently from each other. The positions and orientations of nanotubes inside a layer are chosen at random, with a condition ensuring that the closest distance between surfaces of nanotubes within the layer is larger than a pre-defined minimum distance δ_T . The total number of CNTs in a layer and the choice of the values of δ_L and δ_T are determined by the desired density of the sample.

The approach outlined above makes it possible to generate samples with density as high as 0.6 g/cm^3 . For high density samples, however, the algorithm introduces significant correlations between the orientations of nanotubes in a layer. For example, one can compare the orientations of nanotubes in the top layers of the initial samples shown in Figs. 1a and 2a for densities of 0.023 and 0.2 g/cm^3 , respectively. While the orientation of CNTs is completely random in Fig. 1a, a relatively high degree of orientational anisotropy is apparent in Fig. 2a. The preferential directions of CNT orientations in different layers, however, are different from each other. The random network of bundles, obtained in the dynamic simulations, therefore, does not retain any memory of the preferential directions in the individual planes (Fig. 2d).

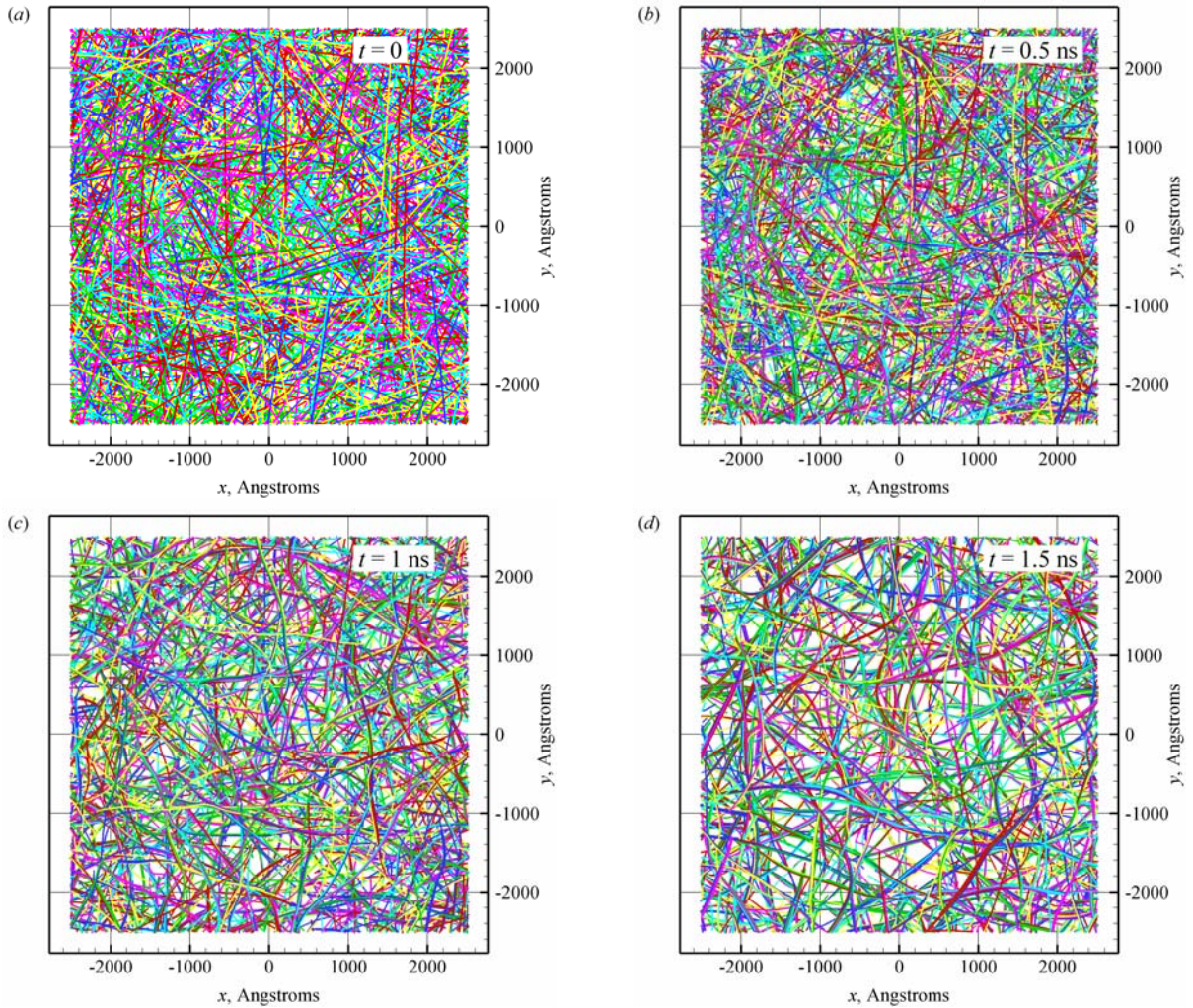


Figure 1. Snapshots from a mesoscopic simulation performed for a system of 1543 (10,10) CNTs with the length of each CNT equal to 200 nm. The dimensions of the system are $500 \text{ nm} \times 500 \text{ nm} \times 175 \text{ nm}$ and the density is 0.023 g/cm^3 . The initial sample is prepared with *Generator II* and the snapshots are shown for times 0 ps (a), 0.5 ns (b), 1 ns (c), and 1.5 ns (d) of the simulation. Different colors correspond to different individual CNTs.

Because all layers in the initial samples are parallel to each other, the network of CNT bundles, generated in a dynamic simulation, can exhibit a certain degree of anisotropy, with preferred orientation of CNT bundles parallel to the planes of the original layers. This anisotropy can be, actually, a desired effect if the goal is to reproduce the structure of a CNT film, where the CNT bundles tend to orient themselves along the underlying substrate. On the other hand, several methods can be introduced in order to increase the degree of the interlayer “mixing” and out-of-plane orientation of the CNTs. For example, after the initial generation of a layer, the nanotubes can be randomly

inclined with respect to the plane of the layer (the maximal inclination angle should still satisfy the restriction on the minimum distance between the CNT surfaces discussed above). Also, an extra kinetic energy can be introduced into the system by assigning initial random velocities to nanotube nodes, resulting in a more active motions and higher degree of randomization at the second (dynamic) stage of the sample preparation (see Section III).

In this work, however, we show that the entangled structure of CNT bundles can be obtained even with the simplest initial samples, where all tubes lay in parallel planes and the initial velocities of all nodes are set to zero. In this case, a relatively small initial inter-tube interaction energy is found to be sufficient to trigger a vigorous evolution of the structure of the CNT material in a constant-energy simulation, leading to the formation of a realistic structure of CNT bundles.

Using *Generator II*, an initial sample can be prepared for simulations with either free or periodic boundary conditions in any of the three directions. The type of the boundary conditions for the directions parallel to the initial layers of CNTs should be specified before the generation of the initial sample, whereas the conditions in the direction normal to the layers can be defined at the stage of the dynamic simulation.

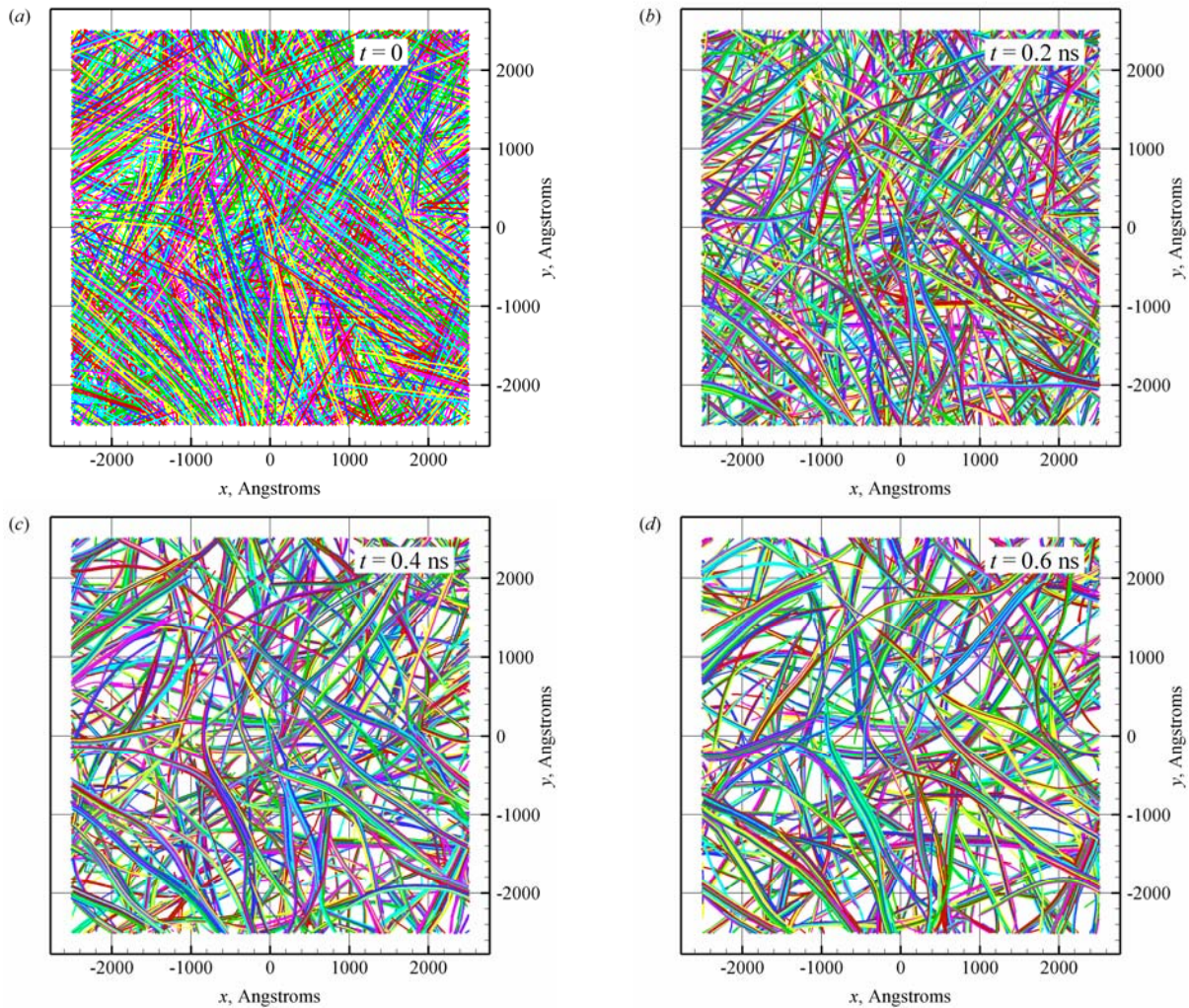


Figure 2. Snapshots from a mesoscopic simulation performed for a system of 1543 (10,10) CNTs with the length of each CNT equal to 200 nm. The dimensions of the system are 500 nm \times 500 nm \times 20 nm and the density is 0.2 g/cm³. The initial sample is prepared with *Generator II* and the snapshots are shown for times 0 ps (a), 0.2 ns (b), 0.4 ns (c), and 0.6 ns (d) of the simulation. Different colors correspond to different individual CNTs.

V. Computational results and discussion

In this section, several examples of self-assembly of nanotubes into a random network of CNT bundles are presented. The initial distributions of CNTs are generated by *Generator II* (an example of self-assembly of CNTs in a sample created by *Generator I* can be found in Ref. 17). All calculations are performed for samples with 200 nm (10,10) nanotubes ($R_T=6.785$ Å). Every nanotube is discretized into 100 segments of equal length. At the initial time $t = 0$, the velocities of all CNT nodes are set to zero. The mesoscopic dynamic simulations are then performed under conditions of constant energy and constant volume. Periodic boundary conditions are applied in the directions parallel to the initial layers of CNTs (denoted as x and y axes). In order to maintain constant volume during the simulations, the samples are placed between two planes perpendicular to the layers (z axis). The planes are exerting additional forces on the CNTs within the sample.

The calculations are performed for three CNT samples having the following dimensions and densities: 500 nm \times 500 nm \times 175 nm and 0.023 g/cm³ (Fig. 1), 500 nm \times 500 nm \times 20 nm and 0.2 g/cm³ (Fig. 2), and 500 nm \times 500 nm \times 200 nm and 0.2 g/cm³ (Fig. 6). The first two samples consist of 1543 CNTs, and the third one consists of 15430 CNTs. In all samples, the parameters defining the initial inter-layer separation and the minimum distance between surfaces of CNTs within the layers are $\delta_L = 3$ Å and $\delta_T = 2.8$ Å, respectively.

As can be seen from Figs. 1 and 2, the process of CNT self-assembly into a network of bundles takes place in both samples. The duration of the process and the parameters of the bundles, however, depend on the density of the material. In the case of a low density of 0.023 g/cm³, the formation of bundles takes place on the time scale of nanoseconds. The mobility of individual tubes remains relatively high even at the time exceeding 1 ns, as can be seen by comparing the snapshots from the simulation taken at 1 ns (Fig. 1c) and 1.5 ns (Fig. 1d). An enlarged side view (along the x axis) of a part of the sample obtained in this simulation at 1.5 ns is shown in Fig. 3. In this image one can see a significant degree of interlayer mixing, i.e. the positions of nodes in the same nanotube in z -direction differ from each other much more than the initial inter-layer separation of $2R_T + \delta_L$. At the same time, a typical inclination of a CNT with respect to the xy plane is not large and the sample has a pronounced anisotropy in z -direction. The degree of interlayer mixing and the inclination angles of nanotubes with respect to the xy plane continue to

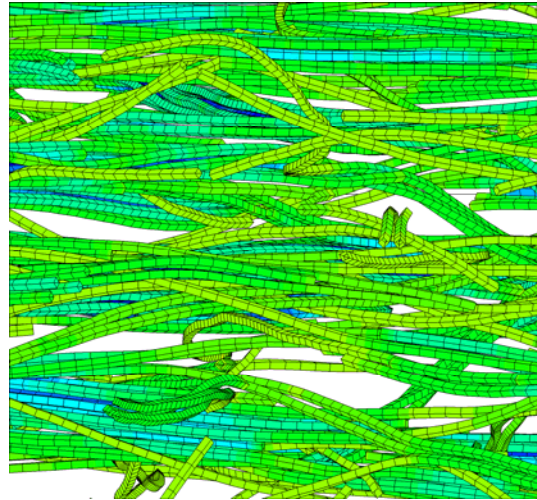


Figure 3. An enlarged view of a part of the sample shown in Fig. 1d, illustrating the degree of inter-layer mixing among the tubes. The view is shown along the x axis. The initial inter-layer separation is equal to 16.57 Å, while the thickness of CNTs in the plot corresponds to their diameter, 13.57 Å. The CNTs are colored according to the local inter-tube interaction energy (blue corresponds to a low energy realized for parallel tubes in a bundle, while green corresponds to a higher interaction energy).

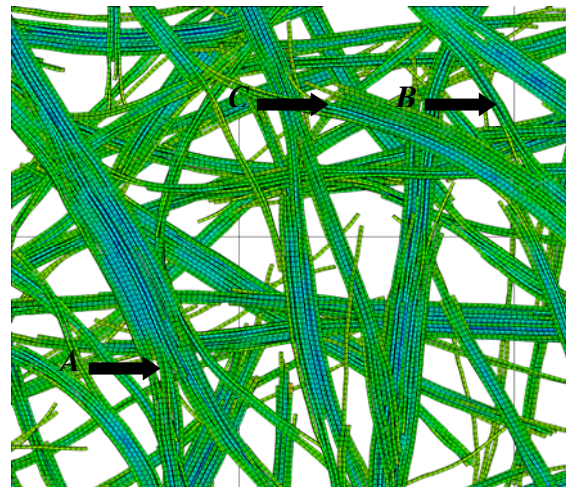


Figure 4. An enlarged view of a part of the sample shown in Fig. 2d, illustrating the arrangement of individual tubes in the bundles. Labels A, B, and C point to places of splitting of a bundle, interconnection between two bundles, and alignment of CNT ends at an end of a bundle, respectively. The coloring scheme is the same as in Fig. 3.

increase as the simulation extends beyond 1.5 ns.

In the case of a larger density of 0.2 g/cm^3 , the formation of bundles is much faster and takes place on a time scale of hundreds of picoseconds. Indeed, the structure of thick bundles, generated by 0.4 ns (Fig. 2c) undergoes much slower changes at a later time, with the evolution of the sample between 0.4 and 0.6 ns being mostly defined by the rearrangements of the remaining individual tubes, as they move to join the existing bundles. Despite the significant slowing down of the rate of the structural changes in the system after the first nanosecond, continuation of the simulation at room temperature for 18 more nanoseconds reveals that the structure of the bundles continues to evolve. The primary direction of the long-term structural evolution is the coarsening of the bundles, which proceeds by thin bundles and individual nanotubes joining the thicker bundles. The growing bundles are also straightening themselves up, reducing the total bending energy in the system. The observation of the continuing changes in the system on the time-scale of tens of nanoseconds is in agreement with relatively large vibrations of CNTs caused by thermal fluctuations observed in experiments²⁹ performed at room temperature. In simulations, a quasi-static network of CNT bundles, where the rate of changes is negligible on the time scale of nanoseconds, can be obtained by decreasing the temperature of the simulations. At the same time, several factors can inhibit the thermal motion, resulting in a quasi-static bundle structure even at room temperature. Among them are the static friction forces (partially related to the presence of CNT defects and cross-links), preventing the sliding of nanotubes inside the bundles, as well as a larger length of the nanotubes, resulting in a more entangled and stable structure of bundles. The investigation of the effect of these factors on the stability of the networks of CNT bundles is a subject of our current work.

A detailed analysis of the arrangement of individual CNTs in the bundles allows us to identify several characteristic structural features in the network of CNT bundles. Some of the structural elements of the network are shown in Fig. 4, namely, a splitting of a thick bundle (A), an inter-connection formed by nanotubes that belong to two different bundles (B), and an alignment of CNT ends at an end of a bundle (C). These features are also observed experimentally, in the images of surface structure of bucky paper and CNT films.^{12-15,18,19}

The evolution of the kinetic energy and different components of the potential energy of the system in the constant energy simulations discussed above is shown in Fig. 5. As expected from the visual analysis of the structural changes in the samples, the system shown in Fig. 2d is close to a quasi-static structure and the energy components in Fig. 5b are exhibiting signs of saturation by the time of 0.6 ns. The process of the bundle formation in the sample shown in Fig. 1, on the other hand, is still far from its completion, and the energy redistribution in the system still continues at the end of the simulation (Fig. 5a). Note, that the energy of the inter-tube interaction, U_{Int} ,

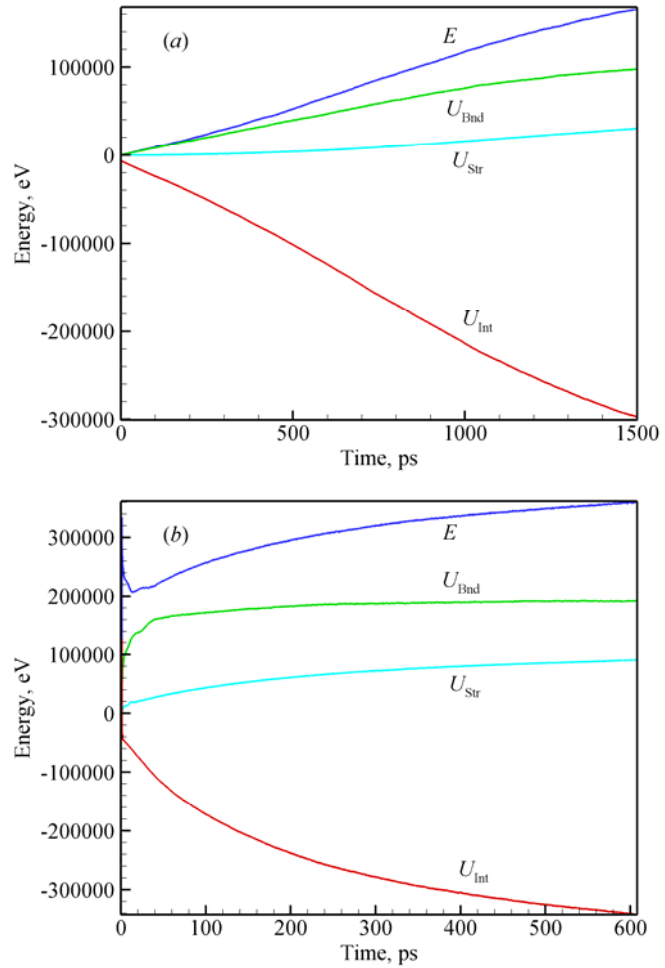


Figure 5. Variation of the kinetic, E , stretching, U_{Str} , bending, U_{Bnd} , and inter-tube interaction U_{Int} energies in the simulations of the CNTs samples illustrated in Figs. 1 and 2. Plot shown in (a) corresponds to Fig. 1 and plot shown in (b) corresponds to Fig. 2.

includes a contribution from the potential energy of the interaction between CNTs and the planes bounding the sample in z -direction.

A snapshot from a simulation performed for a sample with ten times larger, as compared to the system illustrated in Fig. 2, size in z -direction and the same density of 0.2 g/cm^3 is shown in Fig. 6. The parameters used in the generation of the initial sample, as well as the conditions of the dynamic simulation are the same as in the simulation performed for a thinner sample. As a result, the network of CNT bundles shown in Fig. 6 has structural characteristics similar to the ones observed for a comparable time in Fig. 2b.

VI. Summary

A computational approach for generation of a random network of interconnected CNT bundles in CNT-based materials is developed and tested. It includes the generation of an initial distribution of individual CNTs, followed by the dynamic mesoscopic simulation leading to the spontaneous self-assembly of CNTs into a network of bundles. The CNT structures generated in the simulations are visually similar to the ones observed experimentally for CNT films and mats. The development of quantitative parameters, appropriate for structural characterization of the random networks of CNT bundles, as well as the analysis of the structure-properties relationship in the CNT-based materials are subjects of our current work.

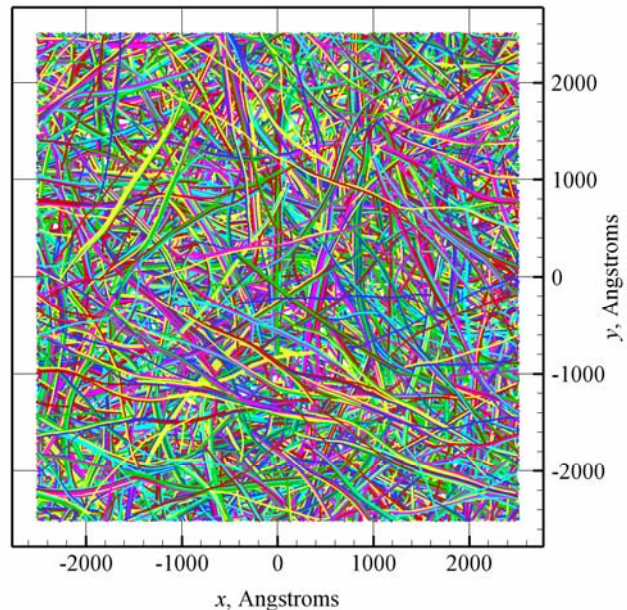


Figure 6. Snapshot taken at a time of 0.25 ns in a mesoscopic simulation performed for a system of 15430 (10,10) CNTs with the length of each CNT equal to 200 nm. The dimensions of the system are 500 nm \times 500 nm \times 200 nm and the density is 0.2 g/cm^3 . Different colors correspond to different individual CNTs.

Acknowledgments

This work was supported by NASA through the Hypersonics project of the Fundamental Aeronautics program (NNX07AC41A), and by the National Science Foundation (NIRT-0403876).

References

- ¹Schonfeld, J. E., Ellerby, D. T., and Arnold, J. O., "An Integrated Thermal and Radiation Protection Shield," *Proc. 16th Annual NASA Space Radiation Investigators' Workshop*, Port Jefferson, New York, May 15–18, 2005.
- ²Vaia, R., and Giannelis, E., "Polymer Nanocomposites: Status and Opportunities," *MRS Bulletin*, Vol. 26, 2001, p. 394.
- ³Vaia, R. A., and Krishna-moorti, R. (ed.), *Polymer Nanocomposites*, American Chemical Society, Washington, DC, 2001.
- ⁴Srivastava, D., Wei, C., and Cho, K., "Nano-mechanics of Carbon Nanotubes and Composites," *Appl. Mech. Rev.*, Vol. 56, 2003, pp. 215–229.
- ⁵Hu, Y. H., Shenderova, O. A., Hu, Z., Padgett, C. W., and Brenner, D. W., "Carbon Nanostructures for Advanced Composites," *Rep. Prog. Phys.*, Vol. 69, 2006, pp. 1847–1895.
- ⁶Yeh, M. K., Tai, N. H., and Liu, J. H., "Dynamic Mechanical Properties of MWNTs/Phenolic Nanocomposites," *Key Engineering Materials*, Vol. 306-308, 2006, pp. 1073–1078.
- ⁷Hastings, D. E., and Garrett, H. B., *Spacecraft-Environment Interactions*, Cambridge University Press, Cambridge, England, U.K., 1996, pp. 142–206.
- ⁸Lai, S. T., Murad, E., and McNeil, W. J., "Hazards of Hypervelocity Impacts on Spacecraft," *Journal of Spacecraft and Rockets*, Vol. 39, 2002, pp. 106–114.
- ⁹Wei, C. Y., and Srivastava, D., "Theory of Transport of Long Polymer Molecules through Carbon Nanotube Channels," *Phys. Rev. Lett.*, Vol. 91, 2003, 235901.

- ¹⁰ Ni, B., Sinnott, S. B., Mikulski, P. T., and Harrison, J. A., “Compression of Carbon Nanotubes Filled with C-60, CH₄, or Ne: Predictions from Molecular Dynamics Simulations,” *Phys. Rev. Lett.*, Vol. 88, 2002, 205505.
- ¹¹ Thess, A., Lee, R., Nikolaev, P., Dai, H., Petit, P., Robert, J., Xu, Ch., Lee, Y. H., Kim, S. G., Rinzler, A. G., Colbert, D. T., Scuseria G. E., Tomanek, D., Fischer, J. E., and Smalley, R. E., “Crystalline Ropes of Metallic Carbon Nanotubes,” *Science*, Vol. 273, 1996, pp. 483–487.
- ¹² Liu, J., Rinzler, G., Dai, H., Hafner, J. H., Bradley, R. K., Boul, P. J., Lu, A., Iverson, T., Shelimov, K., Huffman, C. B., Rodriguez-Macias, F. J., Shon, Y.-S., Lee, T. R., Colbert, D. T., Smalley, R. E., “Fullerene Pipes,” *Science*, Vol. 280, 1998, pp. 1253–1256.
- ¹³ Rinzler, A. G., Liu, J., Dai, H., Nikolaev, P., Huffman, C. B., Rodriguez-Macias, F. J., Boul, P. J., Lu, A. H., Heymann, D., Colbert, D. T., Lee, R. S., Fischer, J. E., Rao, A. M., Eklund, P. C., and Smalley, R. E., “Large-Scale Purification of Single-Wall Carbon Nanotubes: Process, Product, and Characterization,” *Appl. Phys. A*, Vol. 67, 1998, pp. 29–37.
- ¹⁴ Berhan, L., Yi, Y. B., Sastry, A. M., Munoz, E., Selvidge, M., and Baughman, R., “Mechanical Properties of Nanotube Sheets: Alteration in Joint Morphology and Achievable Moduli in Manufactured Material,” *J. Appl. Phys.*, Vol. 95, 2004, pp. 4335–4345.
- ¹⁵ Berhan, L., Yi, Y. B. and Sastry, A. M., “Effect of Nanorope Waviness on the Effective Moduli of Nanotube Sheets,” *J. Appl. Phys.*, Vol. 95, 2004, pp. 5027–5034.
- ¹⁶ Zhigilei, L. V., Wei, C., and Srivastava, D., “Mesoscopic Model for Dynamic Simulations of Carbon Nanotubes,” *Phys. Rev. B*, Vol. 71, 2005, 165417.
- ¹⁷ Volkov, A. N., Simov, K. R., and Zhigilei L. V., “Meso-Scopic Model for Simulation of CNT-based Materials,” *Proc. ASME International Mechanical Engineering Congress and Exposition IMECE2008*, October 31 – November 6, 2008, Boston, Massachusetts, USA, ASME Paper IMECE2008-68021.
- ¹⁸ Sreekumar, T. V., Liu, T., Kumar, S., Ericson, L. M., Hauge, R. H., and Smalley, R. E., “Single-Wall Carbon Nanotube Films,” *Chem. Mater.*, Vol. 15, 2003, pp. 175–178.
- ¹⁹ Ma, W., Song, L., Yang, R., Zhang, T., Zhao, Y., Sun, L., Ren, Y., Liu, D., Liu, L., Shen, J., Zhang, Zh., Xiang, Y., Zhou, W., and Xie, S., “Directly Synthesized Strong, Highly Conducting, Transparent Single-Walled Carbon Nanotube Films,” *Nanoletters*, Vol. 7, 2007, pp. 2307–2311.
- ²⁰ Poulin, P., Vigolo, B., and Launois, P., “Films and Fibers of Oriented Single Wall Nanotubes,” *Carbon*, Vol. 40, 2002, pp. 1741–1749.
- ²¹ Srivastava, D., and Lawson, J. W., “Formation and Structure of Amorphous Carbon Char from Polymer Materials,” *Phys. Rev. B*, Vol. 77, 2008, 144209.
- ²² Volkov, A. N., and Zhigilei, L. V., “Tubular Potential Method for Mesoscopic Simulation of Systems Composed of Carbon Nanotubes or Other Nano-/Micro-tubular Structural Elements,” (to be published).
- ²³ Brenner, D. W., “Empirical Potential for Hydrocarbons for Use in Simulating the Chemical Vapor Deposition of Diamond Films,” *Phys. Rev. B*, Vol. 42, 1990, pp. 9458–9471.
- ²⁴ Brenner, D. W., Shenderova, O. A., Harrison, J. A., Stuart, S. J., Ni, B., and Sinnott, S. B., “A Second-generation Reactive Empirical Bond Order (REBO) Potential Energy Expression for Hydrocarbons,” *J. Phys. Cond. Matt.*, Vol. 14, 2002, pp. 783–802.
- ²⁵ Girifalco, L. A., Hodak, M., and Lee, R. S., “Carbon Nanotubes, Buckyballs, Ropes and a Universal Graphitic Potential,” *Phys. Rev. B*, Vol. 62, 2000, 13104.
- ²⁶ Sun, C.-H., Yin, L.-C., Li, F., Lu, G.-Q., and Cheng, H.-M., “Van der Waals Interactions between Two Parallel Infinitely Long Single-walled Nanotubes,” *Chem. Phys. Lett.*, Vol. 403, 2005, pp. 343–346.
- ²⁷ Stuart, S. J., Tutein, A. B., and Harrison, J. A., “A Reactive Potential for Hydrocarbons with Intermolecular Interactions,” *J. Chem. Phys.*, Vol. 112, 2002, pp. 6472–6486.
- ²⁸ Yi, Y. B., Berhan, L., and Sastry, A. M., “Statistical Geometry of Random Fibrous Networks, Revisited: Waviness, Dimensionality, and Percolation,” *J. Appl. Phys.*, Vol. 96, 2004, pp. 1318–1327.
- ²⁹ Treacy, M. M. J., Ebbesen, T. W., and Gibson, J. M., “Exceptionally High Young’s Modulus Observed for Individual Carbon Nanotubes,” *Nature*, Vol. 381, 1996, pp. 678–680.